Geography and human relationships, vol7, no4, Winter 2025, pp:768-787

Patterning the Heavy, Erosive, and Widespread Rainfalls of the Northwest of Iran by the Factor Analysis Technique

Ali Shahi[1], **Bromand Salahi**[2*]

[1] Associate Professor Department of Rural Development and Extension, College of Agriculture, Tabriz University, Tabriz, Islamic Republic of Iran.

kazemiyeh@tabrizu.ac.ir

[2] Ph.D student Department of Rural Development and Extension, College of Agriculture, Tabriz University, Tabriz, Islamic Republic of Iran.

[3] MSc Department of Agricultural Economic, College of Agriculture, Tabriz University, Tabriz, Islamic Republic of Iran.

Submit date: 2024.22.03 accept date: 2024.14.06

Abstract

This research aim is to identify the dynamic and thermodynamic patterns of heavy and widespread rainfall in northwest of Iran in the period 2000-2019. The percentile method was used to determine heavy rainfall. In dynamic and thermodynamic patterning of heavy rains, factor analysis and hierarchical clustering methods were used. After determining heavy rainfall patterns, two representative days were selected and 500Hpa atmospheric maps were drawn and interpreted. Then, in the GIS software, the heavy rains in the northwest of Iran were zoned. The results showed that in the first pattern, the main factor of air ascent and the occurrence of heavy and widespread rainfall in the northwest of Iran is the Mediterranean cyclone. The presence of a short front in the studied area has increased the intensity of instability, and the establishment of blocking in the mid-level of the atmosphere has caused the strengthening and continuation of precipitation. The results also showed that the main sources of moisture supply for heavy rainfall in the northwest of Iran are the Black Sea and the Mediterranean Sea. The synoptic maps of the representative day of the second pattern showed that the primary cause of the rise of moist air and the occurrence of heavy rain in the northwest of Iran is the merging of the Sudanian cyclone and the Mediterranean cyclone. The existence of a short front and the blocking has caused the creation of a baroclinic atmosphere and, as a result, the rise of air in the studied area.

Keywords: Cluster Analysis, Factor Analysis, Heavy Rainfall, Northwest of Iran, Synoptic Analysis.

doi: **10.22034/GAHR.2024.449624.2077** ESSN: 2645-3851

Introduction

Precipitation is an essential and influential element of human activities so, it is considered the main base of the researches in all environmental and economic planning. Precipitation changes are an important indicator of climate change (Fu et al., 2016) and to evaluate climate changes in the future, precipitation changes should be considered. The climate is a thermodynamic system that often converts potential energy into kinetic energy (Salahi, 2020). Atmospheric hazards, especially heavy rains, lead to destructive floods and cause many losses in human life (Moghimi, 2014) (Li et al., 2016). Precipitation occurs when moist air and the rising factor exist together (Kaviani and Alijani, 2014). The high humidity of the atmosphere and the injection of moisture through the wind play an essential role in heavy rains (Harnack et.al., 1998). According to the FAO report, Iran ranks tenth in the world in terms of the occurrence of natural disasters, and heavy rains and floods are one of them. Heavy rains are an example of weather extremes (Farajzadeh, 2013), and their occurrence is mainly associated with cyclone systems (Mostafaei et al., 2015).

One of the applications of synoptic climatology is the identification and analysis of heavy rains (Alijani, 2013). By identifying and analyzing synoptic patterns, it is possible to predict heavy and widespread rains. The heaviness of the rainfall mainly depends on the geographical conditions of the area receiving the rainfall (Borzou and Azizi, 2015). One of the widely used techniques in synoptic climatology is the factor analysis technique. This technique is used in modeling synoptic phenomena such as environmental hazards. This technique is used when we face multiple variables (with different measurement units) in modeling synoptic phenomena. In this case, the factor analysis technique is used to reduce the number of variables and categorize them as new factors. The purpose of the factor analysis technique is to reduce the number of variables in favor of the factors. Due to the process of factor analysis, with a small number of factors (linear combinations of the main scores of the observed variables), it is possible to obtain almost all the information obtained by a larger set of variables. Researchers such as Salahi and Alijahan (2013) have used this technique in their studies.

Regarding the synoptic analysis of heavy rain events, different studies have been conducted worldwide. Ahmadi and Jafari (2015), in the synoptic and thermodynamic study of the heavy rainfall of 104 mm leading to the flood of March 14, 2014, in Bandar Abbas city, found the presence of Sudanese low pressure and the expansion of the deep trough over Iran, Iraq, Arabia, and the Red Sea to be effective in causing this rainfall. They also believed that the location of Bandar Abbas city in front of the trough and the presence of vertical movements caused the rise and instability of the air and the occurrence of heavy rain. Ahmadi et al. (2015) in the synoptic and thermodynamic analysis of the rainfall leading to the flood of Alborz province on July 28, 2014, found that cold air in the upper atmosphere, the presence of a trough, moisture injection from the Caspian Sea, low pressure on the land surface and northwesterly currents are the important reasons for the occurrence of this rainfall. They also found that the dominant pattern in sea level before and during the precipitation event is the Pakistan thermal low. Gasemifar et al. (2017) analyzed the synoptic patterns of heavy rainfall in western Iran. Ahmadi and Ahmadi (2018) investigated the heavy rains of more than 50 mm in the south of Iran, in addition to the synoptic analysis of the generating systems of this heavy rain, they also tracked the heavy rains in the south of Iran. Ahmad et al. (2015) classified the synoptic patterns producing heavy rainfall in 5 different regions of Saudi Arabia

during 2000-2014. They showed that the obtained synoptic patterns are different in the lower atmospheric levels but relatively similar in the upper atmospheric levels.
Hoseynisadr et al. (2019) analyzed the synoptic mechanisms of heavy rainfall on Apr 24, 2016, in northwest Iran and found that the presence of moist air and the ascent factor caused by the westerly waves play an important role in the occurrence of heavy rainfall in northwest Iran. Foroutan and Salahi (2020) analyzed the heavy rain of March 19, 2019, in Minodasht City (Iran) and showed that during heavy rain, a high-pressure system formed in Mongolia and South China and created a strong pressure gradient and air front in Minodasht city. They also showed that in the upper levels of the atmosphere, a cut-off low blocking is placed as an obstacle in the way of the westerly winds and caused the westerly winds to enter Minodasht city. Beyranvand et al. (2022) analyzed the heavy rains leading to floods in Apr 2017 in the Boroujerd watershed from a statistical and synoptic view.
Jet streams also play a vital role in the occurrence of heavy rains. The role of the jet stream in the occurrence of extreme rainfall in Iran was investigated by Masodyan and Mohammadi (2011) and Zakizadeh et al. (2018). In different regions of the world, statistical and synoptic analysis of heavy rains has been done by some researchers such as Mannan et al. (2013); Pook et al. (2014); Needham et al. (2015); Akbari et al. (2016); Kamae et al. (2017); Waliser and Guan (2017); Agel et al. (2018); Rabinowitz et al. (2018); Ahmad and William (2018); Espinoza et al. (2018); Eiras-Barca et al. (2018); Lakshmi et al. (2019). Few researches have been done regarding the identification of the sources and moisture paths of Iran's heavy rains. However, researchers such as Gavidel-Rahimi et al. (2014); Mirmosavi et al. (2016); Salamati Hormozi et al. (2017); Khansalari et al. (2017); Shamsipor et al. (2018); Shadmani et al. (2018); Hoseynisadr et al. (2019); Sepandar and Omidvar (2021); Ahadi et al., (2020), and Asghari Saraskanrood and Saeidi (2023) investigated the occurrence of heavy rainfalls from a synoptic view and identified its moisture sources and pathways. Several studies have been done regarding heavy rains and their moisture sources (Pourkarimian et al. 2022; Salahi and Nasiri Qalabiin, 2023; Frotan and Salahi, 2023; Vatanparast et al. 2024). Since it is difficult to prevent the occurrence of climatic hazards such as heavy rainfall, therefore; by identifying the patterns that generate heavy rainfall in each region, it is possible to take the necessary preventive measures to minimize the possible damages and also use the rainfall optimally through their prediction. In the last two decades, North-West Iran has witnessed many heavy rains, and in this article, its productive patterns are examined.

Material and methods

Northwest Iran includes the provinces of West Azarbaijan, East Azarbaijan, Ardabil, North Kurdistan, and West Zanjan (Figure 1). The data used in this research include ground station data and upper atmosphere data for 2000-2019. First, the daily rainfall data of 23 synoptic stations located northwest of Iran were obtained from the Iranian Meteorological Organization (www.irimo.ir). Then, the upper atmosphere data, including daily average sea level pressure, geopotential height, zonal wind, meridian wind, omega, air temperature, relative humidity, and precipitable water for 500hPa level, were obtained from the NCEP/NCAR database. These data can be obtained from the website www.cdc.noaa.gov. The range of the studied area was defined between 0 to 100 degrees east longitude and 10 to 70 degrees north latitude.

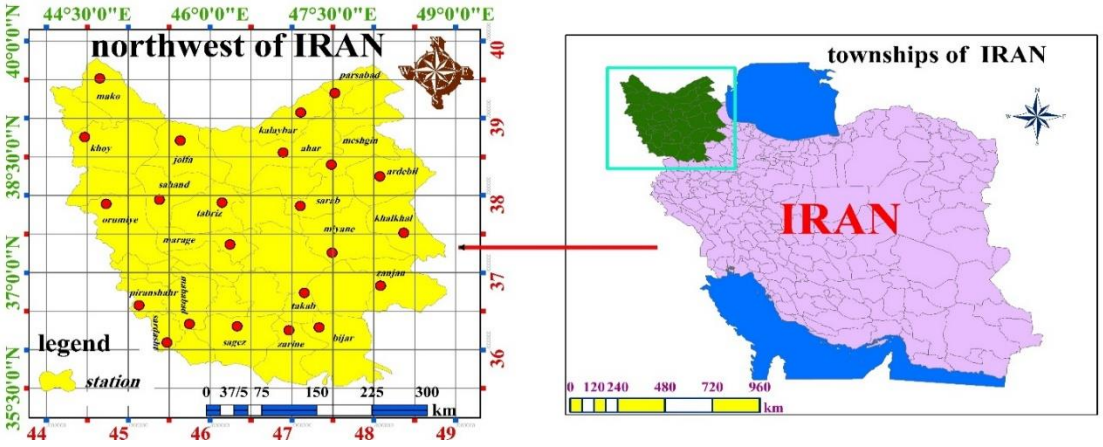

Figure 1. The geographical location of the Northwest of Iran

Researches show that there is no specific criterion for defining heavy rains (Alijani et al., 2010). In most climate studies, heavy rains have been studied in two ways: percentiles and thresholds. Zhang et al. (2005) and Ghasemifar et al. (2017) determined the rainfall in the 99th percentile as heavy rainfall. The 98th and 95th percentiles were considered as heavy rainfall by Seibert et al. (2007) and Sotoudeh and Alijani (2013), respectively. Days with rainfall of more than 30, 94.4, and 50.8 mm per day were introduced by Alijani (2013), Vaida and Kulkarni (2007,) and Groisman et al. (1999) respectively as the thresholds for determining heavy rainfall. The most common method of calculating heavy rains is using the percentile index (Halabiyan and Pourgazi 2015; Alexander et al. 2006). Estimates from trial and error showed that if the percentile is selected above 99 and the area covered by heavy rainfall is more than 30%, the conditions of convergence will provide a suitable justification for heavy rainfall (Mofidi et al. 2007; Alijani et al. 2010; Sotoudeh and Alijani 2013). In this article, the days when at least seven synoptic stations located in the northwest of Iran had at least 20 mm of rain at the same time were selected, and according to this criterion, 27 days of heavy rain were identified. Then, the trend of heavy annual rainfall in the Northwest of Iran was drawn by the Excel software. After obtaining the upper atmosphere data from the National Oceanic and Atmospheric Administration (NOAA) website, the factor analysis technique was used to reveal the effective factors in the heavy rains in northwest of Iran. The main aim of the factor analysis technique is to identify unobservable factors based on a set of observable variables. The factor is a new variable that is estimated by the linear combination of the main scores of the observed variables based on Equation 1:

$$Fj=\sum WjiXi=Wj1X1+Wj2X2+\ldots+WjpXp \quad (1)$$

W are factor score coefficients and, P is the number of variables. After carrying out the factor analysis technique and determining the main factors, using hierarchical cluster analysis, heavy rains in northwest Iran were modeled, and two main heavy rain clusters were extracted. The day with heavy rainfall with the most station coverage in each cluster was chosen as the representative day of each pattern. For that day, sea level pressure (SLP), 500 hPa geopotential height (HGT_{500}), Precipitable Water (PW), Relative Humidity (RH), vorticity,

vector wind, V-wind, U-wind, Stream humidity, Air temperature, Omega, the convergence of humidity, Hovmoller diagram, Jetstream, and rainfall zoning maps were drawn and interpreted. Then, with the inverse distance weighting (IDW) interpolation method in the GIS environment, the heavy rains in the northwest of Iran were zoned and analyzed. In the synoptic analysis of environmental hazards such as heavy rainfalls, sea level pressure (SLP), and 500 hPa geopotential height (HGT_{500}) are mainly used. These two variables may not be able to explain the synoptic facts of environmental hazards. So, in this article, in addition to SLP and HGT_{500}, eight other variables such as PW, RH, Vorticity, Vector wind, V-wind, U-wind, Air temperature, and Omega are also used which have been processed with the factor analysis technique, therefore, increasing the number of variables and also considering the coverage of precipitation in the synoptic analysis of heavy rainfalls is one of the innovations of this research.

Results and Discussion

Figure 2 shows the trend of changes in the occurrence of heavy rains in the northwest of Iran. According to this figure, in 2004 and 2014, the occurrence of heavy rains was more than in other years. The trend of changes in the occurrence of heavy rains in the northwest of Iran is almost constant in the long term (it has a very weak downward slope) and indicates the lack of significant changes in the occurrence of this natural hazard from the past until now. Table 1 shows the characteristics of the patterns obtained, including the number and percentage of days of heavy rainfall representative of each pattern. According to this table, 70.37 days with heavy rainfall in the northwest of Iran are included in pattern number 1 and 29.62 in pattern 2.

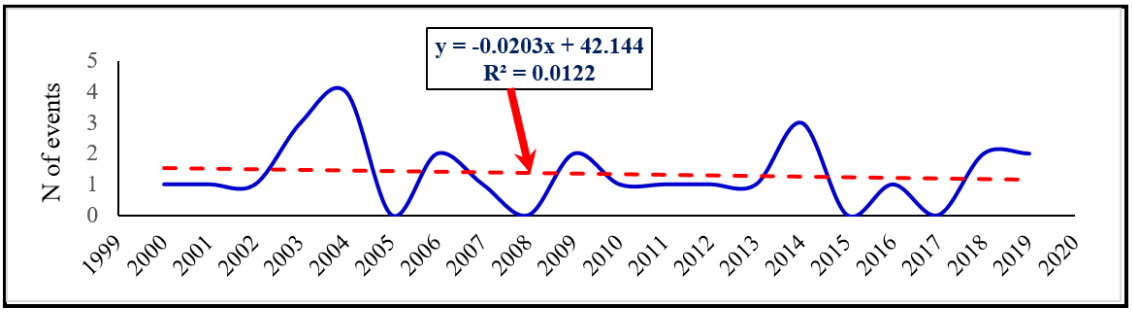

Figure 2. The trend of changes in the occurrence of heavy rains in the northwest of Iran

Table 1. The characteristics of the patterns of days of heavy rainfall in the northwest of Iran

Pattern Number	Percentage of event days of each pattern	Number of event days of each pattern	The representative year of the pattern	The representative month of the pattern	The representative day of the Pattern
1	**70.37**	19	2003	4	16
2	**29.62**	8	2006	2	3

Table 2 shows the results of the Kaiser-Meyer-Olkin (KMO) measure and Bartlett's test of Sphericity. The Kaiser-Meyer-Olkin measure of Sampling Adequacy is 0.628, and the sig value of Bartlett's test of Sphericity is also zero. Kaiser (1974) and Meyer et al. (1977) set the minimum value of KMO to be 0.5 to perform factor analysis, and the implementation of factor analysis is considered unobstructed if KMO is equal to or greater than 0.5. Crany and Kaiser (1977) also determined the value of KMO for factor analysis to be 0.6 or more. Since the KMO value obtained for the investigated variables is 0.628 and the sig value of Bartlett's test of Sphericity is zero, therefore it can be said that the investigated data can be factorized.

Table 2. The KMO and Bartlett's test of Sphericity

Kaiser-Meyer-Olkin Measure of Sampling Adequacy		**.628**
Bartlett's Test of Sphericity	Approx. Chi-Square	259.303
	Df	45
	Sig.	.000

Table 3 shows the total variance explained. According to this table, 84.42% of the total variance of the data is explained by the three obtained factors. If in the factor analysis technique, the total variances explained are greater than 80%, this technique is ideal for modeling (Sharifi, 1994). Considering that 84.42% of the variance of the total data was explained by the three factors obtained, therefore, the factor analysis technique performed well in reducing the number of variables and was able to explain a large percentage of the variances.

Table 3. Total Variance Explained

Component	Initial Eigenvalues			Extraction Sums of Squared Loadings			Rotation Sums of Squared Loadings		
	Total	% of Variance	Cumulative %	Total	% of Variance	Cumulative %	Total	% of Variance	Cumulative %
1	4.795	47.951	47.951	4.795	47.951	47.951	3.219	32.189	32.189
2	2.115	21.145	69.096	2.115	21.145	69.096	2.930	29.303	61.492
3	1.532	15.324	84.421	1.532	15.324	84.421	2.293	22.928	**84.421**

Figure 3 shows the scree plot of factor scores. Based on this figure, factors 1 to 3 have performed most in reducing the number of variables and explaining the variances. The decrease in the slope of the graph from factor number 4 to 10 shows that these factors are less effective in explaining the variances. Using the factor analysis method, three factors were extracted. Figure 4 shows the dendrogram of heavy rainfalls in the Northwest of Iran, which was obtained using the hierarchical clustering technique. Based on this figure, the representative days of the first and second patterns, which had the highest explained variance and the highest percentage of heavy rainfall coverage in the northwest of Iran, were analyzed synoptically.

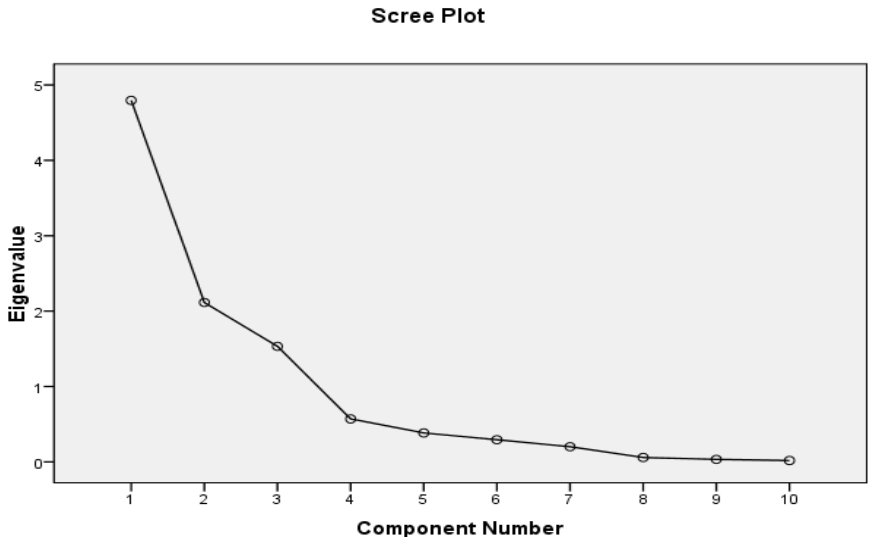

Figure 3. Scree plot

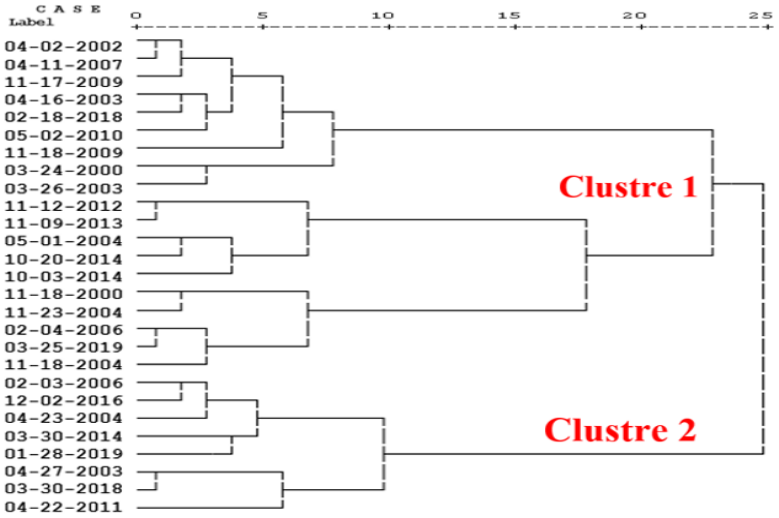

Figure 4. The dendrogram of heavy rainfalls in the Northwest of Iran

Synopsis analysis of the representative day of the first pattern (Apr 16, 2003)

Apr 16, 2003, was chosen as the representative day of the first pattern. Table 4, shows the characteristics of the representative day of the first pattern. In this table, Mean daily temperature (c), mean daily relative humidity (%), cloudiness (octas), and daily rain (mm) are shown for the synoptic stations of the northwest of Iran that have daily rainfall of more than 20 (15 stations). Figure 5 shows the zoning of daily rainfall for Apr 16, 2003, in the northwest of Iran. According to this figure, the maximum heavy rainfall occurred on the mentioned day in the western parts of the study area, and the maximum heavy rainfall was recorded at Urmia station in the amount of 44 mm.

4. Characteristics of the representative day of the first pattern (Apr 16, 2003) Table

Variables / Stations	Mean Daily Temperature (c)	Mean Daily Relative Humidity (%)	Cloudiness (Octas)	Daily Rain (mm)
Miyane	5.8	86	8	31
Zanjan	7.1	82.8	8	31.9
Bijar	7.5	83	6	20
Tekab	7.2	81.8	5.5	23
Zarine	4.1	96	5.4	21
Sarab	0.6	92.8	8	20
Sardasht	6.8	89.7	7.1	24
Piranshahr	6.7	89.4	7.8	38
Orumiye	**5.6**	**89.1**	**7.75**	**44**
Ahar	0.6	92.8	8	20
Mahabad	7.2	86.3	7.5	28.7
Marage	7	78	6.5	27
Khoy	5.4	86.3	8	34.6
Kaleybar	0.2	96.6	8	32
Parsabad	7.5	83	6	20

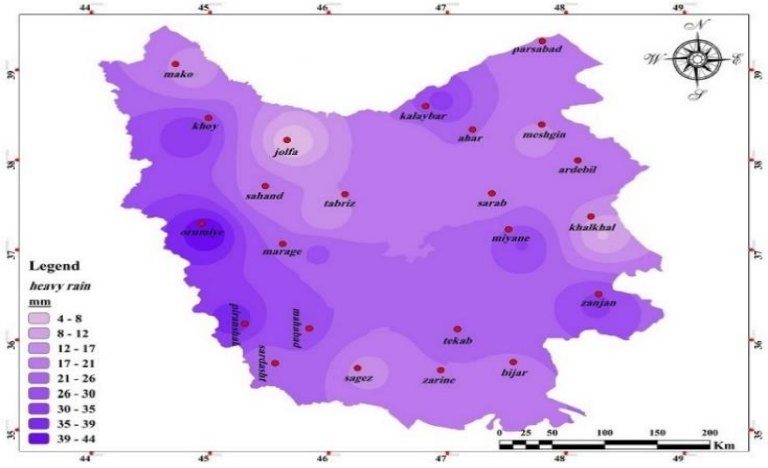

Figure 5. Zoning of daily rainfall for Apr 16, 2003, in the northwest of Iran

Figure 6 shows sea level pressure (hPa) and 500hPa geopotential height maps in the studied area for Apr 16, 2003. Based on this figure, a low-pressure core with a central pressure of 1007.5 hPa has formed over the Arabian Peninsula. The 1015 hPa tongue of this low-pressure system is extended to the west and northwest of Iran. The counter-clockwise air movement in this low-pressure system has caused moist south and southwest currents to blow to the northwest of Iran. In the north of Aral Lake, a strong high-pressure system has formed, and its central pressure has reached 1047.5 hPa. The southwest tongues of this high-pressure system have moved to the northwest of Iran and caused cold air to enter this region. The

clockwise movement of the air in the mentioned high-pressure system has caused northeasterly currents to blow to the studied area.
These winds, passing over the Caspian Sea, became humid and penetrated to the northwest of Iran, bringing moisture to this region. The intrusion of the high-pressure 1022.5 hPa tongues from the northeast and the intrusion of the 1015 hPa low-pressure tongue from the southwest have caused the formation of a landfront in the northwest of Iran. The collision of these two tongues has led to the advection of warm and humid southern air over the cold northern air. It has led to an increase in air cloudiness and heavy rainfall in the northwest of Iran so that, on Apr 16, 2003, at least 15 synoptic stations in the northwest of Iran received more than 20 mm of rain in one day. Figure 6 also shows that at the level of 500 hPa, a strong cold front with a central height of 5600 meters has formed over Iraq and has become a blocking system. This blocking system has caused the westerly currents to slow down the air continues to rise and heavy rains occur in the northwest of Iran. Northwest of Iran on Apr 16, 2003, has been placed in front of the westerly winds. In front of the trough of the westerly winds, there is a positive vorticity advection, which provides the conditions for the lower convergence and upper divergence of the air mass; in this case, atmospheric instability increases and leads to heavy precipitation. Figure 7 shows that due to the presence of a cut-off low in the west of the studied area (over Iraq), a negative omega nucleus with a value of -0.5 p/s has formed at the 500 hPa level, and it shows that the atmosphere of the northwest of Iran is unstable. Figure 7 also shows that at the 500 hPa level, the vorticity is positive, which indicates the presence of conditions necessary for moist air to rise and cause heavy rainfall. Figure 8 indicates that the air temperature at the 500 hPa level is about -20 degrees Celsius. This figure also shows that the dominant currents in northwest of Iran at 500 hPa level are the southwest currents, which are in the same direction and coordinated with the south and southwest currents of the sea surface. Figure 9 shows that on Apr 16, 2003, precipitable water in the northwest of Iran reached more than 90 kg/m2, which indicates the high potential of the atmosphere of the northwest of Iran to cause heavy rainfall on this day. This figure also shows that the relative humidity of the air in the northwest of Iran is high. Figure 10 shows the convergence and divergence of humidity in northwest of Iran on Apr 16, 2003. According to this figure, the convergence of moist air is observed in the northwest of Iran, which has led to the rise of air and heavy rainfall.

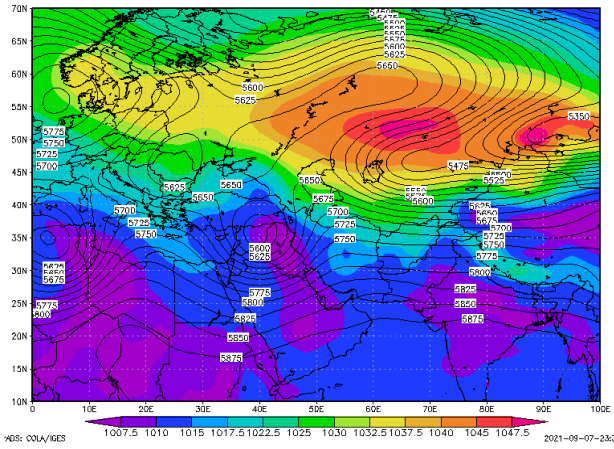

Figure 6. Sea level pressure (color) and 500 hPa geopotential height (curve), for Apr 16, 2003

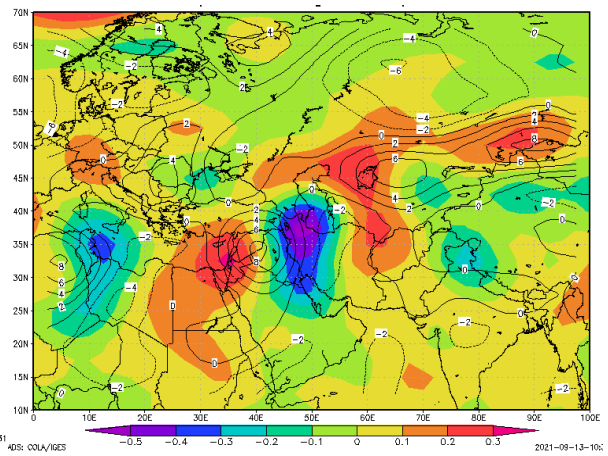

Figure 7. Omega (color) and Vorticity (curve) at 500 hPa for Apr 16, 2003

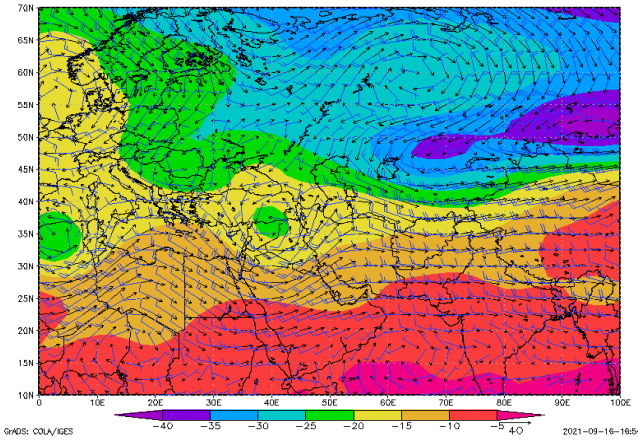

Figure 8. Air temperature (color) and Vector wind (curve) at 500 hPa, for Apr 16, 2003

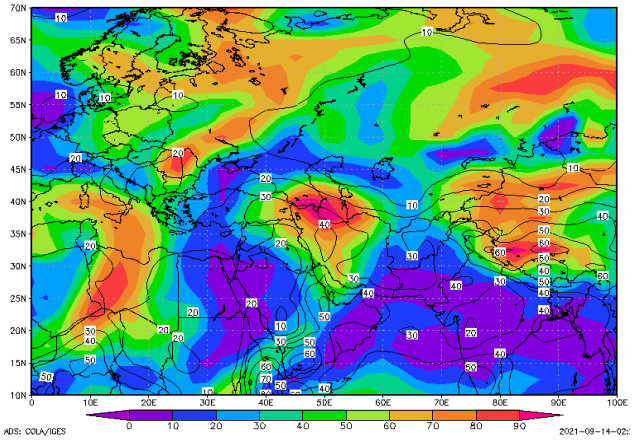

Figure 9. Precipitable water (color) and Relative humidity (curve), at 500 hPa, for

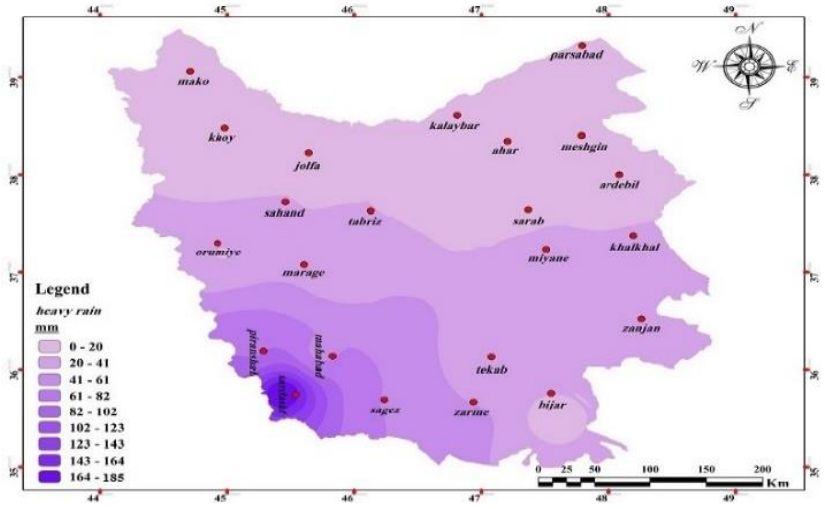

Figure 10. Convergence and Divergence of humidity (color) and stream humidity (curve), at 500 hPa, for Apr 16, 2003

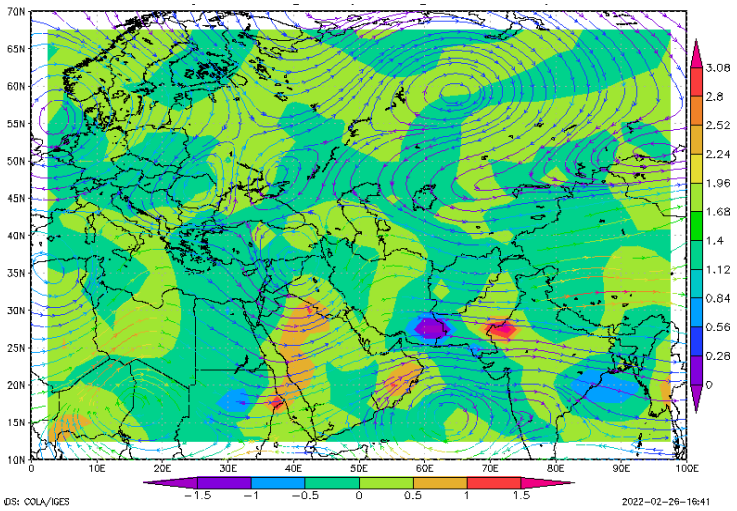

Figure 11. Zoning of daily rainfall for Feb 03, 2006, in the northwest of Iran

Synopsis analysis of the representative day of the second pattern (Feb 03, 2006)

Table 5 shows the characteristics of a representative day of the second pattern. Feb 03, 2006, was chosen as the representative day of the second pattern. In this table, as in Table 4, some weather variables are shown for the synoptic stations of the northwest of Iran that have daily rainfall of more than 20 nm (14 stations). Figure 11 shows the zoning of daily rainfall for Feb 03, 2006, in the northwest of Iran. According to this figure, the maximum heavy rainfall on Feb 03, 2006, increased from the northeast to the southwest and reached the highest amount (185 mm) at the Sardasht station.

5. Characteristics of the representative day of the second pattern (Feb 03, 2006) Table

Variables / Stations	Mean Daily Temperature (c)	Mean Daily Relative Humidity (%)	Cloudiness (Octas)	Daily Rain (mm)
Miyane	1	95.8	8	34
Zanjan	1.5	91.2	8	27
Tekab	2.2	94.6	7.8	20.8
Zarine	0.1	95.5	8	44.9
Khalkhal	3.5	96.6	8	34
Sagez	3.2	91.1	8	61
Sarab	1.5	93.5	8	20
Sardasht	**2.5**	**97.2**	**8**	**185**
Piranshahr	1.7	96.6	8	80
Orumiye	0.4	95.1	8	20
Mahabad	3.3	89	7.7	57
Marage	3.9	88.2	8	28
Tabriz	2.2	89.2	7.7	24.2
Sahand	1.3	90.7	7.7	21.01

Figure 12 shows the sea level pressure and geopotential height of 500 hPa on Feb 03, 2006. As seen from this figure, the 1012.5 hPa low-pressure tongue located over the Red Sea covers the northwest of Iran. The counterclockwise rotation of the air in this system has caused the transfer of moist air from the Red Sea and the Mediterranean Sea to the northwest of Iran. The penetration of this tongue has caused the instability of the air in the northwest of Iran and has provided the conditions for the rise of moist air and the creation of heavy rain. On this day, at the 500 hPa level of the atmosphere, a deep trough can be seen, whose axis extends from the northwest of the Caspian Sea to the south of Libya. The direction of the axis of this trough is northwest-southeast. This trough, in Western Europe, houses a cut-off low, whose central height has reached 5025 meters. Under the mentioned cut-off low, the curves of the iso-hypes have been stretched towards the southern latitudes and have created a strong trough. The axis of this secondary trough extends from the center of Türkiye to the south of Libya. The topography of the 500 hPa level of the atmosphere shows that on the right side of the mentioned trough, the curves of the iso-hypes have become more compact and the wind speed has increased at the 500 hPa level. On the other hand, the location of the northwest of Iran in front of the westerly winds shows the unstable atmosphere on Feb 03,2006, in the northwest of Iran. This instability can also be seen in Figure 13. In this figure, over the northwest of Iran, a negative omega core can be seen, which indicates the baroclinic atmosphere at the 500 hPa level of the atmosphere.

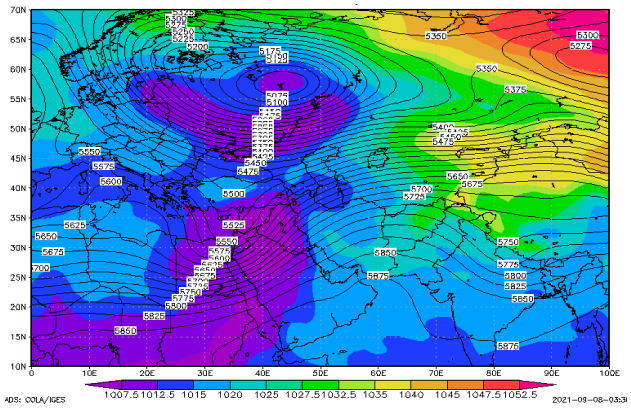

Figure 12. Sea level pressure (color) and 500 hPa geopotential height (curve), for Feb 03, 2006

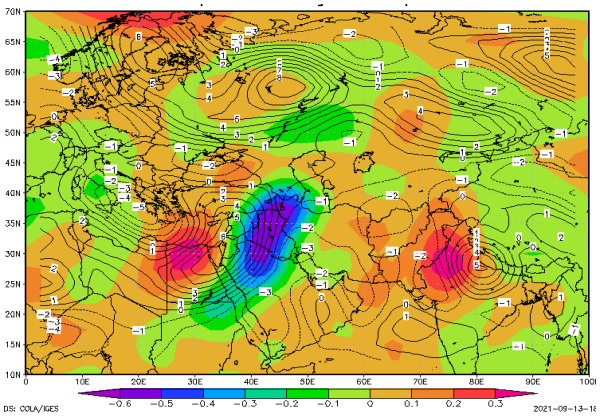

Figure 13. Omega (color) and Vorticity (curve) at 500 hPa for Apr 16, 2003

The values of the vorticity in the studied area fluctuate between zero and one, which indicates a positive vorticity advection in the northwest of Iran. Since the representative day of the second pattern is in winter, the Northwest of Iran witnessed a temperature of -15 to -20 degrees Celsius at the level of 500 hPa on Feb 03, 2006 (Figure 14). The wind direction of 500 hPa level on Feb 03, 2006, was from the southwest to the northeast, which led to the transfer of moisture from the Red Sea and the Mediterranean Sea to the studied area (Figure 14). Figure 15 shows that at the 500 hPa level of the atmosphere, precipitable water and relative air humidity are appropriate and can lead to heavy precipitation if other conditions exist. Figure 16 also indicates that the humid air current in the study area causes the transfer of moist air from the moisture sources of the west of Iran (Red Sea and Mediterranean Sea) to the study area. In terms of moisture convergence, the environmental conditions for air ascent and transformation moisture are ready for heavy rainfall.

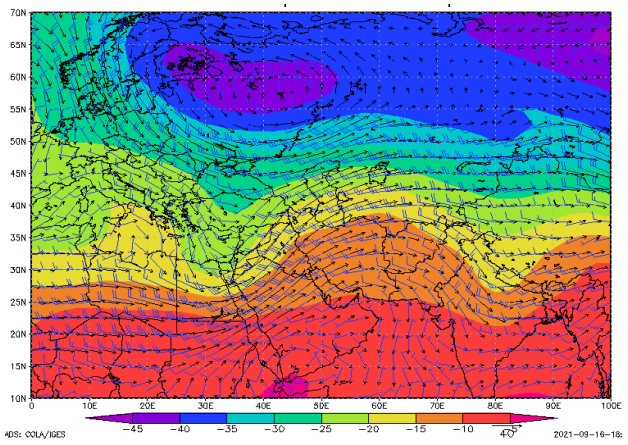

Figure 14. Air temperature (color) and Vector wind (curve) at 500 hPa, for Apr 16,

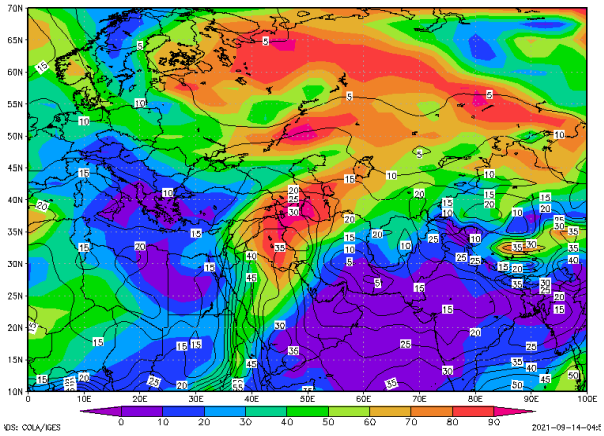

Figure 15. Precipitable water (color) and Relative humidity (curve), at 500 hPa, for

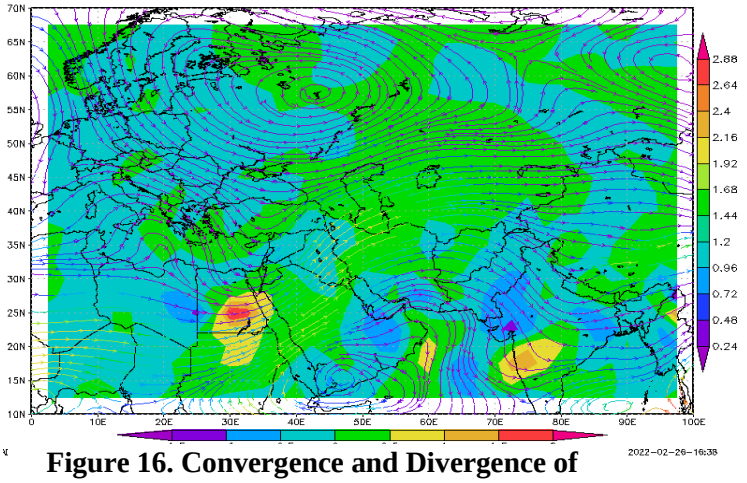

Figure 16. Convergence and Divergence of humidity (color) and stream humidity (curve),

Conclusion

The results showed that spring, autumn, and winter have the most occurrences of heavy rains in the northwest of Iran, and in the spring season, the most occurrences of heavy rains belong to April. The trend of changes in the occurrence of heavy rains in the northwest of Iran is stable in the long term, which indicates the lack of significant changes in the occurrence of heavy rains in the northwest of Iran over time. The statistics obtained from the factor analysis technique showed that this technique has an excellent ability to reduce the number of synoptic variables and produce climatic factors. It has been able to pattern the heavy rains of northwest Iran along with hierarchical cluster analysis. The analysis of the representative days of the first and second patterns showed that the heavy rains in the northwest of Iran from 2000 to 2019 were associated with the formation of a strong cyclone system and the presence of a short front on the surface of the earth. This finding is consistent with the results of the studies of Mostafaei et al. (2015), Kaviani and Alijani (2014), Ahmad and William (2018), Carla-Lima et al. (2009), Pook et al. (2014), Agel et al. (2018) and Barth and Steinkohl (2004). The results also showed that in the middle level of the atmosphere, the establishment of the deep trough system, along with blocking and the location of the studied area in the eastern half of the trough (under the front of the trough axis), along with the values of positive vorticity and negative omega, has caused heavy rainfall in the northwest of Iran. This result is also in agreement with the findings of Mohammadi and Masodyan (2010), (2016), Azizi (2011), Dargahian et al. (2014); Salamati Hormazi et al. (2017), Foroutan and Salahi (2020), Beyranvand et al. (2022), Akbari et al. (2016), and Sánchez-Almodóvar et al. (2022). This research showed that at the 500 hPa level of the atmosphere, the density of the curves of the iso-hyps indicates the presence of the jetstream, which has caused the ascent to intensify and strengthen the heavy rainfall. This result is in line with the findings of Salahi and Alijahan (2013), Kaviani and Alijani (2014), Shamsipour et al. (2018), and, Zakizadeh et al. (2018). Local conditions in spring and autumn have led to heavy rainfall in the studied area, which is consistent with the results of studies by Alijani (2013) and (2019), and Nie and Sun (2021). This research indicated that the convergence of the maximum humidity in the direction of the western winds entering the study area with the intensification of the humidity had strengthened the heavy rainfall. This result is also consistent with the research results of Lakshmi et al. (2019), Hu et al. (2022), Shadmani et al. (2018), and Alijani (2013), who consider the humidity factor to be more important than the ascension factor for causing heavy rains.

References

Agel, L., M. Barlow, F. Colby, H. Binder, J. Catto, A. Hoell, J. Cohen, 2018. Dynamical analysis of extreme precipitation in the US Northeast based on large-scale meteorological patterns. Journal of Climate Dynamics Springer-Verlag GmbH Germany, part of Springer Nature, 152(392); 1-22. https://doi.org/10.1007/s00382-018-4223-2.

Ahadi, M., B. Zeynali., A. Hossini Sadr., & Siah Sarani, A, 2020. Synoptic Investigation of heavy rainfall led to flooding on January 11, 2020 in southern Sistan and Baluchestan. Physical Geography Quarterly, 13(50); 1-14.

Ahmad, E.S., A.G. William, 2018. A classification of Synoptic patterns inducing heavy precipitation in Saudi Arabia during the period 2000-2014. The Journal of Atmosfera, 31; 47-67. DOI: 10.20937/atm.2018.31.01.04.

Ahmadi, H., M. Baaghideh, S. Asadi, F. Ahmadi, 2015. Analysis of Extreme Rainfall Event Resulting in Floods on June 28th, 1394 in Alborz Province. Environmental Hazards Management, 2(4); 451-469. DOI: 10.22059/jhsci.2015.58274. (In Persian).

Ahmadi, M., F. Jafari, 2015. Super heavy rainfall, 104mm,on 14 identification of synoptic and thermodynamic of March 2014 manufactures destructive flood in Bandarabbas Township. Environmental Hazards Management, 2(3); 307-324. DOI: 10.22059/jhsci.2015.56069. (In Persian).

Ahmadi, M., F. Jafari, 2018. Full routing and synoptic analysis a sample of studies of heavy rainfall systems in excess of 50 mm in southern Iran. Journal of Spatial Analysis Environmental Hazards, 5(3); 83-102. DOI:10.29252/jsaeh.5.3.83. (In Persian).

Akbari-Azirani, T., G. Azizi, A. Asadi, M. Davoudi, 2016. The role of blocking system in heavy precipitation of Iran (a case study: southeast of Iran January 2008). Arabian Journal of Geosciences, 9(11); 591. DOI: 10.1007/s12517-016-2588-2.

Alexander, L. V., 23Co-authors, 2006. Global observed changes in daily climate extremes of temperature and precipitation. Journal of Geophysical Research: Atmospheres, 111(D5); 109. DOI: 10.1029/2005J D006290.

Alijani, B. 2013. Iran's climate. Payam Noor University Publications, Tehran. (In Persian).

Alijani, B. 2013. Synoptic Climatology. Samt Publications, Tehran. (In Persian).

Alijani, B., M. Khosravi, M. Esmailnejad, 2010. A synoptic analysis of January 6, 2008 heavy precipitation in the southeast of Iran. Journal of Climate Research, 1(3-4); 3-14. (In Persian).

Asghari Saraskanrood, S., & A. Saeidi, 2023. Investigation of the Effect of Land Use Change on Runoff of Qarachai River Basin Using HEC-HMS Models. Journal of Geography and Environmental Studies, 12(45); 134-148. Dor: 20.1001.1.20087845.1402.12.45.8.0

Azizi, G., M. Soltani, A. Hanafi, A. Ranjbar, E. Mirzai, 2011. Analysis of the effect of the blocking system in causing heavy precipitations (case study: precipitations from October 25 to 28, 2008 in the northwest of Iran). Geographical researches, 26(103); 117-148. (In Persian).

Barth, H.J., F. Steinkohl, 2004. Origin of Winter Precipitation in the Central Coastal Lowlands of Saudi Arabia. Journal of Arid Environments, 57(1); 101-115. https://doi.org/10.1016/S0140-1963(03)00091-0.

Beyranvand, I., A. Gandomkar, A. Abasi, M. Khodagoli, 2022. Statistical-Synoptic Analysis of April 2019 Heavy Rainfall in Doroud-Boroujerd Basin. Journal of Natural Environmental Hazards, 11(32); 169-188. DOI:10.22111/JNEH.2022.38564.1806. (In Persian).

Borzou, F., G. Azizi, 2015. Suggesting a Simple Criterion to Estimate Heavy Rainfall in Iran. Physical Geography Research, 47(3); 347-365. DOI:10.22059/JPHGR.2015.55335. (In Persian).

Carla-Lima, K., P. Satyamurty, J.P. Reyes-Fernandez, 2009. Large-Scale Atmospheric Conditions Associated With Heavy Rainfall Episodes in Southeast Brazil, Theoretical and Applied Climatology, 101(1-2); 121-135. DOI: 10.1007/s00704-009-0207-9.

Cerny, B.A., H.F. Kaiser, 1977. A study of a measure of sampling adequacy for factor-analytic correlation matrices. Multivariate Behavioral Research, 12(1); 43-47. https://doi.org/10.1207/s15327906mbr1201_3.

Dargahian, F., B. Alijani, H. Mohamadi, 2016. Synoptic Analysis of Blockings Causing Heavy and Continuous Rains in Iran. Journal of Geography and Environmental Hazards, 3(2); 155-173. DOI:10.22067/GEO.V3I2.26653. (In Persian).

Eiras-Barca, J., N. Lorenzo, J. Taboada, A. Robles, G. Miguez-Macho, 2018. On the relationship between atmospheric rivers, weather types, and floods in Galicia (NW Spain). Natural Hazards and Earth System Sciences, 18(6); 1633–1645. https://doi.org/10.5194/nhess-18-1633-2018.

Espinoza, V., D.E. Waliser, B. Guan, D.A. Lavers, F.M. Ralph, 2018. Global Analysis of Climate Change Projection Effects on Atmospheric Rivers. Geophysical Research Letters, 45(9); 4299–4308. DOI: 10.1029/2017GL076968.

Farajzadeh, M. 2013. Climatic Hazards of Iran. Samt Publications, Tehran. (In Persian).

Foroutan, M., B. Salahi, 2021. Synoptic analysis of heavy rainfall on March 19, 2017, in Minoodasht City. Journal of Geography and Environmental Hazards, 9(4); 163-180. DOI:10.22067/GEOEH.2021.67780.1003. (In Persian).

Frotan, M., Salahi, B. (2023). Analyzing the relationship between heavy rains and extreme winds in Ardabil province. Geography and Human Relationships, 5(4); 128-146. doi: 10.22034/gahr.2023.382739.1799. (In Persian).

Fu, Y., F. Chen, G. Liu, Y. Yang, R. Yuan, R. Li, Q. Liu, Y. Wang, L. Sun, 2016. Recent trends of Summer Convective and Strati form Precipitation in Mid-Eastern China. Scientific Reports, 6(33044); 1-8. DOI: 10.1038/srep33044.

Gavidel-Rahimi, Y., M. Ahmadi, D. Hatami-Zarne, M. Rezai, 2014. Identification of synoptic patterns of heavy rainfall manufacturers destructive floods in Jiroft city. Geography (Sheffield, England), 41(12); 161-178. (In Persian).

Ghasemifar, E., S. Naserpour, L. Arezomandi, 2017. Analysis of synoptic patterns related to extreme precipitation over west of Iran. Journal of Spatial Analysis of Environmental Hazards, 4(2); 69-86. https://jsaeh.khu.ac.ir/article-1-2717-en.html. (In Persian).

Groisman, P.Y., T.R. Karl, D.R. Easterling, R.W. Knight, 1999. Ganges in the probability of heavy precipitation: important indicators of climatic change. Climatic change, 42(1); 243-283. DOI: 10.1023/A: 1005432803188

Halabiyan, A.H., F. Pourjazi, 2016. Synoptic Analysis of Climatic Hazards in Southwestern Iran (Case study: flood generating heavy precipitation of Azar 1391). Journal of Spatial Analysis Environmental Hazards, 2(4); 31-46. https://jsaeh.khu.ac.ir/article-1-2530-en.html. (In Persian).

Harnack, R.P., D.T. Jensen, J.R. Cermak, 1998. Investigation of upper-air conditions occurring with heavy summer rain in Utah. International Journal of Climatology, 18(7); 701–723. https://doi.org/10.1002/(SICI)1097-0088(19980615)18:7<701::AID-JOC265>3.0.CO;2-S.

Hoseynisadr, A., G.H. Mhamadi, F. Abdolalizade, V. Khojastegolami, 2020. Analysis of Synoptic Mechanisms of Heavy Rainfall of 14th of April 2017 in Northwest Iran. Journal of Geography and Planning, 23(70); 79-100. https://geoplanning.tabrizu.ac.ir/article_10096.html?lang=en. (In Persian).

Hu, P., W. Chen, Z. Li, SH. Chen, L. Wang, Y. Liu, 2022. Close Linkage of the South China Sea Summer Monsoon Onset and Extreme Rainfall in May over Southeast Asia: Role of the Synoptic-Scale Systems. Journal of Climate, 35(13); 4347– 4362. DOI:10.1175/JCLI-D-21-0740.1.

Kaiser, H.F. 1974. An index of factorial simplicity. Psychometrika, 39(1); 31–36. https://doi.org/10.1007/BF02291575.

Kamae, Y., W. Mei, S.P. Xie, M. Naoi, H. Ueda, 2017. Atmospheric rivers over the Northwestern Pacific: Climatology and interannual variability. Journal of Climate, 30(15); 5605-5619. DOI:10.1175/JCLI-D-16-0875.1

Kaviyani, M., B. Alijani, 2014. The Basics Climatology. Samt Publications, Tehran. (In Persian).

Khansalari, S., A. Moheb-olhoje, T. Razii, F. Ahmadi-givi, 2017. Identification of atmospheric circulation patterns responsible for significant precipitation events with cold weather anomaly in Tehran: A comparison of two circulation classification methods. Journal of the Earth and Space Physics, 43(2); 369-384. DOI:10.22059/JESPHYS.2017.57884. (In Persian).

Lakshmi, D.D., A.N.V. Satyanarayana, A. Chakraborty, 2019. Assessment of heavy precipitation events associated with floods due to strong moisture transport during summer monsoon over India. Journal of Atmospheric and Solar-Terrestrial Physics, 189; 123-140. https://doi.org/10.1016/j.jastp.2019.04.013.

Li, Z., S. Yang, B. He, C. Hu, 2016. Intensified Springtime Deep Convection over the South China Sea and the Philippine Sea Dries Southern China. Scientific Reports, 6(30470); 1-9. DOI: 10.1038/srep30470.

Mannan, M., M. Chowdhuryc, S. Karmakar, 2013. Application of NWP model in prediction of heavy rainfall in Bangladesh. Procedia Engineering, 56; 667-675. https://doi.org/10.1016/j.proeng.2013.03.176.

Masoodian, A., B. Mohammadi, 2011. Analysis of Jet Stream Frequencies Associated with Super Heavy Rainfalls of Iran. Iran-Water Resources Research, 7(2); 80-91. https://www.iwrr.ir/article_16185.html?lang=en. (In Persian).

Meyer, E.P., H.F. Kaiser, B.A. Cerny, B.F. Green, 1977. MSA for a special Spearman matrix. Psychometrika, 42; 153-156.

Mirmosavi, H., M. Doustkamian, F. Setode, 2016. Analyzing Spatial Autocorrelation Patterns of Heavy and Super Heavy Showers of Iran. Geography and environmental planning, 27(3); 67-86. DOI:10.22108/GEP.2017.97958. (In Persian).

Mofidi, A., A. Zarin, G.H. Janbaz-Gobadi, 2008. Determining the synoptic pattern of autumn heavy and extreme precipitations on the southern coast of the Caspian Sea. Journal of the Earth and Space Physics, 33(3); 131-154. (In Persian).

Mogimi, E. 2014. Knowledge of risks for a better quality of life and a more sustainable environment. Tehran University Publications, Tehran. (In Persian).

Mohammadi, B., S.A. Masoodian, 2010. Synoptic Analysis of Heavy Precipitation Events in Iran. Geography and Development, 8(19); 47-70. DOI:10.22111/GDIJ.2010.1108. (In Persian).

Mostafaei, H., B. Alijani, M. Saligheh, 2016. Synoptic Analysis of Widespread Heavy Rains in Iran. Journal of Spatial Analysis Environmental Hazards, 2(4); 65-76. DOI:10.18869/acadpub.jsaeh.2.4.65. (In Persian).

Needham, H.F., B.D. Keim, D. Sathiaraj, 2015. A review of tropical cyclone-generated storm surges: Global data sources, observations, and impacts. Reviews of Geophysics, 53(2); 545-591. DOI: 10.1002/2014RG000477

Nie, Y., J. Sun, 2021. Synoptic-Scale Circulation Precursors of Extreme Precipitation Events Over Southwest China During the Rainy Season. Journal of Geophysical Research Atmospheres, 126(13). https://doi.org/10.1029/2021JD035134.

Pook, M.J., J.S. Risbey, C.C. Ummenhofer, P.R. Briggs, T.J. Cohen, 2014. A Synoptic climatology of heavy rain events in the Lake Eyre and Frome catchments. Frontiers in Environmental Science, 2(54); 1-8. https://doi.org/10.3389/fenvs.2014.00054.

Pourkarimian, A., Soyuf Jahromi, M., Malakooti, H. (2022). Investigation and study of flood moisture transfer (Case study: March 2017 in south and southwest of Iran). Amphibious Science and Technology, 2(4), 40-61. doi: 10.22034/jamst.2022.543537.1050. (In Persian).

Rabinowitz, J.L., A.R. Lupo, P.E. Guinan, 2018. Evaluating Linkages between Atmospheric Blocking Patterns and Heavy Rainfall Events across the North-Central Mississippi River Valley for Different ENSO Phases. Advances in Meteorology, 2018; 1-8. https://doi.org/10.1155/2018/1217830

Salahi, B. 2020. Thunderstorms. Mohaghegh Ardabili University Publications, Ardabil. (In Persian).

Salahi, B., M. Alijahan, 2013. Synoptic Analysis of Climatic Hazards in Yasouj Municipality: a case study of an Episode of Heavy Rain on 11th March 2011. Journal of Geography and Environmental Hazards, 2(1); 73-90. DOI:10.22067/GEO.V2I1.18679. (In Persian).

Salahi, B., Nasiri Qalabiin, S. (2023). Modeling and synoptic analysis of thunderstorms in the coastal area of Gilan. Amphibious Science and Technology, doi: 10.22034/jamst.2023.544244.1122. (In Persian).

Salamati-Hormozi, V., K. Omidvar, R. Kavosi, M. Hamzenejad, 2017.Recognition and Analysis Synoptic-dynamical Analysis of Flood Circulation Patterns in Ilam and Lorestan Provinces (Aban, 1394). Nivar, 41(96-97); 9-27. https://doi.org/10.30467/nivar.2017.48071. (In Persian).

Sánchez-Almodóvar, E., J. Martin-Vide, J. Olcina-Cantos, M. Lemus-Canovas, 2022. Are Atmospheric Situations Now More Favorable for Heavy Rainfall in the Spanish Mediterranean? Analysis of Episodes in the Alicante Province (1981–2020). Atmosphere, 13(9). https://doi.org/10.3390/atmos13091410.

Seibert, P., A. Frank, H. Formayer, 2007. Synoptic and regional patterns of heavy precipitation in Austria. Theoretical and Applied Climatology, 87(1); 139-153. DOI: 10.1007/s00704-006-0198-8.

Sepandar, N., K. Omidvar, 2021. Investigation of the Relation between South and Southwest Iran's Heavy Rainfall with Atmospheric Rivers (ARs). Journal of Applied Research in Geographical Sciences, 21(61); 295-314. DOI:10.52547/jgs.21.61.295. (In Persian).

Shadmani, L., M.A. Nasre-esfahani, A.R. Gasemi, 2018. Determination of humidity sources and accurate trajectory of moist air mass effective on heavy rainfalls in west and south of Iran (case study: flooding events of October and November 2015). Iranian Journal of Geophysics, 12(2); 50-63. DOR: 20.1001.1.20080336.1397.12.2.4.5. (In Persian).

Shamsipour, A.A., S. Kaki, S.M. Jasemi, A. Jafari, 2018. Synoptic and Thermodynamic Analysis of Heavy Rainfall in the West and Southwest of Iran. (Case Study: 12-15 April 2016). Geography and Planning, 22(64); 149-167. https://geoplanning.tabrizu.ac.ir/article_7884.html?lang=en. (In Persian).

Sharifi, H.P. 1994. The principles of psychometrics and psych testing. Roshd publications, Tehran. (In Persian).

Sotoudeh, F., B. Alijani, 2015. The Relationship between Spatial Distribution of Heavy Precipitation and Pressure Patterns in Guilan Province. Journal of Spatial Analysis Environmental Hazards, 2(1); 63-73. DOI: 10.18869/acadpub.jsaeh.2.1.63. (In Persian).

Tolabineshad, M., Z. Hejazizade, M. Salige, 2020. Spatial Distribution of blocking systems and its Coincidence to the Cold Seasons wet year in Iran. Journal of Geography, 17(62); 20-40. (In Persian).

Vaidia, S.S., J.R. Kulkarni, 2007. Simulation of heavy precipitation over Santacruz, Mumbai on 26 July 2005, using Mesoscale model. Meteorology and Atmospheric Physics, 98; 55-66. https://link.springer.com/article/10.1007/s00703-006-0233-4.

Vatanparast, F., Sobhani, B., Zali Korabasloo, A. (2024). Synoptic-thermodynamic analysis of heavy rainfall patterns in Kermanshah province (case study: period 2010 to 2019). Geography and Human Relationships, doi: 10.22034/gahr.2023.419298.1955. (In Persian).

Waliser, D., B. Guan, 2017. Extreme winds and precipitation during landfall of atmospheric rivers. Nature Geoscience, 10(3); 179-183. DOI: 10.1038/ngeo2894.

Zaki zadeh, M.B., M. Salige, M.H. Naserzade, M. Akbari, 2018. Statistical analysis and synoptic most effective jet stream pattern creating the precipitation of Iran. Journal of Natural Environmental Hazards, 7(15); 31-48. DOI:10.22111/JNEH.2017.3335. (In Persian).

Zhang, X., 23Co-authors, 2005. Trends in Middle East climate extreme indices from 1950 to 2003. Journal of Geophysical Research Atmospheres, 110(D22). DOI: 10.1029/2005JD006181.